行政院國家科學委員會專題研究計畫　成果報告

亂流突暴現象對非均勻砂礫啟動機率之影響

計畫類別：個別型計畫
計畫編號：NSC93-2211-E-002-022-
執行期間：93 年 08 月 01 日至 94 年 10 月 31 日
執行單位：國立臺灣大學生物環境系統工程學系暨研究所

計畫主持人：吳富春

報告類型：精簡報告
報告附件：出席國際會議研究心得報告及發表論文
處理方式：本計畫可公開查詢

中　華　民　國 95 年 1 月 16 日

行政院國家科學委員會專題研究計畫成果報告

亂流突暴現象對非均勻砂礫啟動機率之影響

Effect of turbulent bursting on entrainment probability of nonuniform sediment

計畫編號：NSC 93-2211-E-002-022

執行期限：93 年 8 月 1 日至 94 年 10 月 31 日

主持人：吳富春　國立台灣大學生物環境系統工程學系

中文摘要

本研究探討近床有序流結構對非均勻砂礫啟動機率之影響。本研究利用四階 Gram-Charlier 機率密度函數(GC pdf)描述近床流速隨機分布，並納入亂流突暴之高階相關性係數。本研究結果較先前之常態與對數常態分布模式結果具有更高之精確度，可用來預測均勻或非均勻粒徑砂礫在部分運移與全運移情況之啟動機率。本研究結果亦顯示在粗糙河床時三階 GC pdf 可替代四階 GC pdf，但在光滑河床時須使用四階 GC pdf 納入高階相關性之影響。

關鍵詞：啟動機率，亂流突暴，近床有序流結構，非均勻砂礫。

Abstract

The effects of near-bed coherent flow structures on the entrainment probabilities of mixed-size sediment are investigated in this study. The 4th-order Gram-Charlier probability density function (GC pdf) of near-bed streamwise velocity is employed to account for the higher-order correlations associated with turbulent bursting. As compared to the previous models using normal and lognormal pdfs, the present results demonstrate significantly improved agreement with the observed data for the unisize and mixed-size sediments under partial- and full-transport conditions. The results also reveal that for fully rough beds the 3rd-order GC pdf approximates the 4th-order one, however, for smooth beds the 4th-order GC pdf must be used to capture the effects of higher-order correlations.

Keywords: Entrainment probability, turbulent bursting, near-bed coherent flow structures, mixed-size sediment.

1. Introduction

In this study we investigate the effects of near-bed coherent flow structures on entrainment probabilities of mixed-size sediments. A compilation of experimental and numerical data for a wide range of hydraulic roughness is used to parameterize the higher-order (2nd-, 3rd-, and 4th-order) correlations associated with turbulent bursting. The model predictions are broadly compared with the experimental data for unisize and mixed-size sediments under full- and partial-transport conditions. Some new insights into the process of sediment entrainment are provided.

2. Near-Bed Coherent Flow Structures

The near-bed coherent flow structures vary as a function of the height y^+ ($=u_* y/\nu$) and roughness k_s^+ ($=u_* k_s/\nu$), where $y=$ distance from mean bed level, $u_*=$ shear velocity, $\nu=$ kinematic viscosity, and $k_s=$ roughness height. Generally, the turbulence intensity σ_u (2nd-order moment) increases with y^+ in the vicinity of the bed surface, reaches its maximum value at a distance from the bed and then decreases with y^+; the skewness factor S_u (3rd-order

moment) is positive in the vicinity of the bed surface, but becomes negative as y^+ increases; the flatness (or kurtosis) factor F_u (4th-order moment) decreases with y^+ in the vicinity of the bed surface, reaches its minimum value at a distance from the bed and then increases with y^+. Based on a compilation of experimental and numerical data for a wide range of hydraulic roughness (shown in Figure 1), the higher-order moments at y_c^+ (= near-bed coherent height where the turbulence intensity is maximal) are extracted, and expressed as a function of k_s^+ for smooth and transitional beds:

$$\begin{cases} \sigma_u / u_* = -0.187 \ln(k_s^+) + 2.93 \\ S_u = 0.102 \ln(k_s^+) \\ F_u = 0.136 \ln(k_s^+) + 2.30 \end{cases} \quad \text{for } k_s^+ \le 70 \qquad (1a)$$

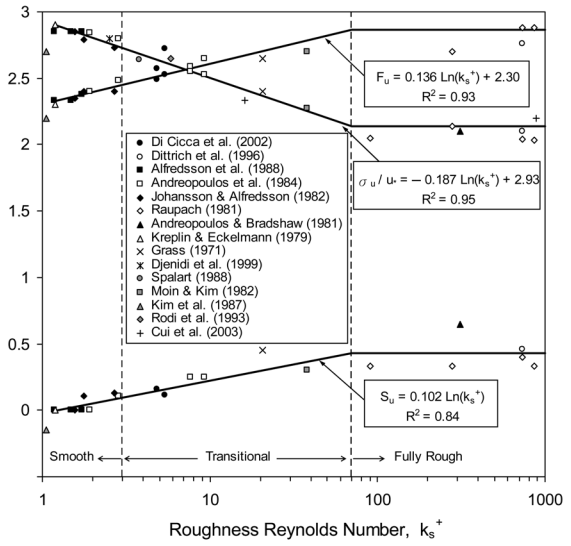

Fig. 1. Variations of 2nd-, 3rd-, and 4th-order moments of streamwise velocity fluctuation with roughness Reynolds number

For fully rough beds, the higher-order moments appear to be independent of k_s^+, i.e.,

$$\begin{cases} \sigma_u / u_* = 2.14 \\ S_u = 0.43 \\ F_u = 2.88 \end{cases} \quad \text{for } k_s^+ > 70 \qquad (1b)$$

Eq. (1) can be used to specify the higher-order moments required for the 4th-order Gram Charlier (GC) pdf of near-bed turbulent velocity, given by

$$f_{GC4}(U) = \frac{\exp(-U^2/2)}{\sqrt{2\pi}} \left[1 + \frac{S_u}{3!}(U^3 - 3U) + \frac{F_u - 3}{4!}(U^4 - 6U^2 + 3) \right] \qquad (2)$$

where $U = u'/\sigma_u$ = normalized velocity fluctuation, in which $u' = u_b - \overline{u}_b$, u_b = near-bed instantaneous streamwise velocity, $\overline{u}_b$ = mean approaching velocity.

3. Computation Procedure

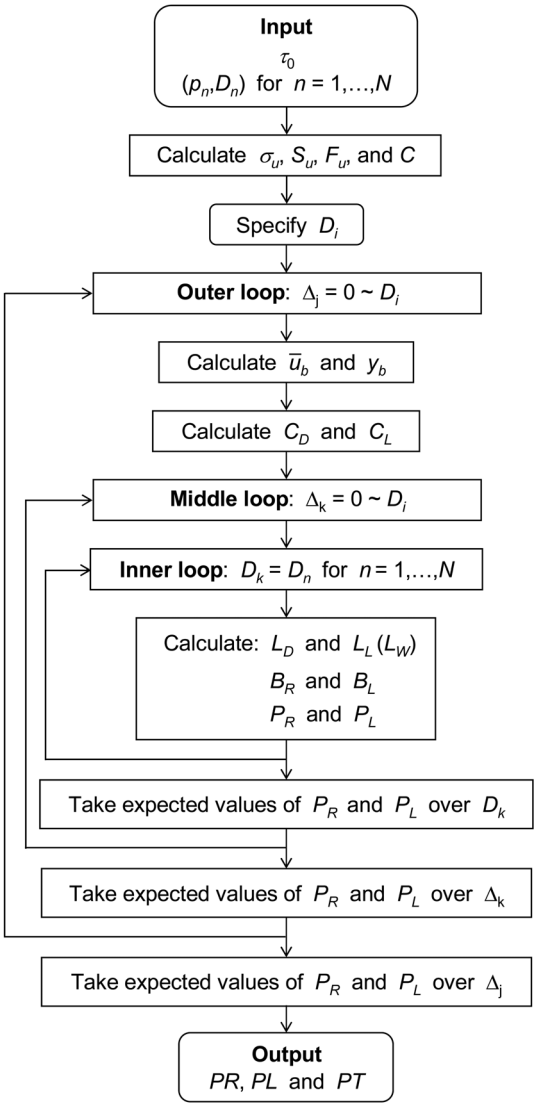

Fig. 2. Triple-loop procedure for computation of entrainment probabilities

Computation of the entrainment probabilities is implemented with a triple-loop procedure. The flowchart is illustrated in Fig. 2, where the outer loop is for the full range of exposure height Δ_j, the middle loop is for the full range of friction height Δ_k, and the inner loop is for the full range of downstream grain size D_k.

4. Results and Discussion

4.1 Entrainment Probabilities

(1) Unisize Sediment

Variations of the lifting probability PL with dimensionless shear stress θ are shown in Fig. 3, where the result of the present model is in good agreement with the data for unisize sediment. The results of three earlier models are also shown in Fig. 3. The present model demonstrates a significant improvement in the prediction of PL, especially for the high value of θ (≈ 1) where the earlier models have a consistent tendency to overestimate PL. By incorporating the 4th-order GC pdf and the random grain protrusion, the present model reduces the magnitudes of PL corresponding to high values of θ, i.e., the effects associated with smaller particle sizes or lower lifting thresholds are more precisely captured.

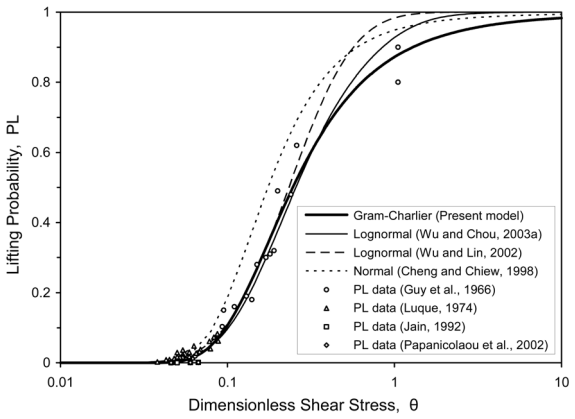

Fig. 3. Variation of lifting probability with dimensionless shear stress for unisize sediment

To quantitatively demonstrate the agreement between the predicted and observed results, the Euclidean norm $\|e\|_2$ (i.e., the root-sum-square of errors) and coefficient of determination R^2 for different models are listed in Table 1, where the values of $\|e\|_2$ and R^2 associated with the present model exhibit significant improvements over those of earlier models, primarily attributed to the additional factors considered in this study.

Table 1. Euclidean norms and coefficients of determination for different models

Entrainment probability model	Euclidean norm, $\|e\|_2$	Coefficient of determination, R^2
Cheng and Chiew (1998)	0.541	0.858
Wu and Lin (2002)	0.266	0.966
Wu and Chou (2003a)	0.245	0.971
Present model	0.209	0.979

(2) Mixed-size Sediment

The present model is further used to compute the total entrainment probabilities PT of mixed-size sediment under partial- and full-transport conditions. A comparison of the predicted and observed PT values is shown in Fig. 4(a), where satisfactory agreement is demonstrated, with a global coefficient of determination $R^2 = 0.971$. The results indicate that the present model is applicable to evaluating the entrainment probabilities of mixed-size sediment under partial- and full-transport conditions. The merit of the present model is further demonstrated by comparing our results with those of two earlier models, one developed for evaluating full transport of mixed-size sediment (Sun and Donahue 2000) and the other for entrainment of unisize sediment (Wu and Chou 2003a). To explore the suitability of the two earlier models to the conditions beyond their original scopes, we

use the Sun-Donahue model to calculate the partial-transport entrainment probabilities [data from Wu and Yang (2004)] and use the Wu-Chou model to compute the entrainment probabilities of mixed-size sediment [data from Sun and Donahue (2000)]. The results are shown in Fig. 4(b), which reveal that the Sun-Donahue model overestimates the entrainment probabilities of partial transport yet the Wu-Chou model consistently underestimates the entrainment probabilities of mixed-size sediment. In view of these, it is clear that the applicability of the earlier models to prediction of the entrainment probabilities for partially transported mixed-size sediment is rather limited.

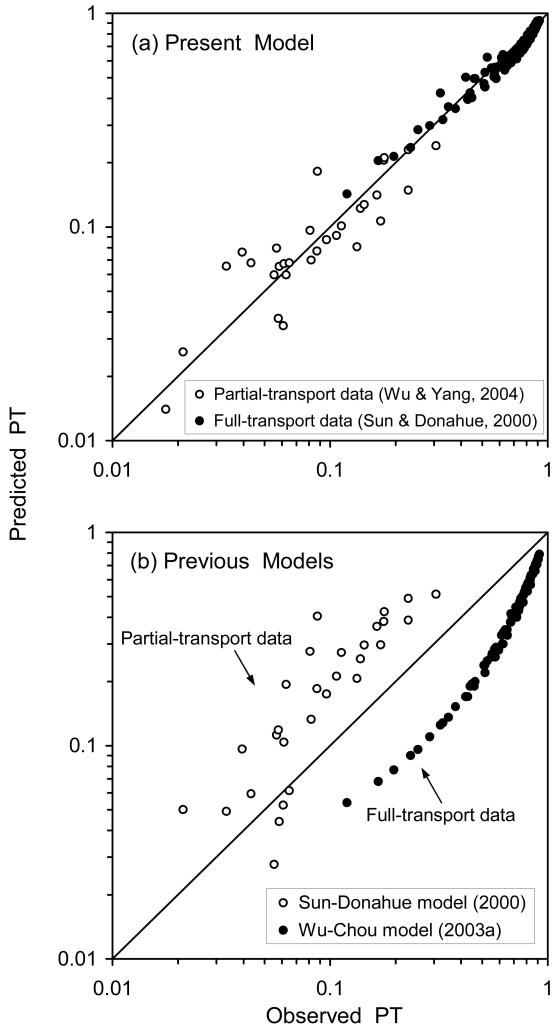

Fig. 4. Comparison of predicted and observed total entrainment probabilities for partial- and full-transport conditions of mixed-size sediment (a) present model (b) two previous models

4.2 Effects of Higher-Order Correlations

To investigate the effects of higher-order correlations on flows over smooth and rough beds, we compare the truncated 2nd-, 3rd-, and 4th-order GC pdfs of u_b, as shown in Fig. 5, where $k_s^+ = 3$ and $k_s = 2$ mm for smooth bed, while $k_s^+ = 100$ and $k_s = 20$ mm for rough bed. The results reveal that for the smooth bed, the 2nd- and 3rd-order GC pdfs are similar to each other but different from the 4th-order one. However, for the rough bed, the 3rd- and 4th-order GC pdfs appear to be identical. These results imply that for rough beds, the 3rd-order GC pdf approximates the 4th-order one. However, for smooth beds, the 4th-order GC pdf must be used to incorporate the effect of higher-order correlations.

It is shown in Fig. 5 that the standard deviation of $f_u(u_b)$ for the smooth bed is smaller than that for the rough bed, indicating that for the rough bed the magnitudes of near-bed velocity fluctuations (or turbulence intensity) are significantly greater. For the smooth bed, the primary difference between the 4th-order GC pdf and normal pdf is in the kurtosis, with the normally distributed u_b more concentrated in the vicinity of $\overline{u}_b$; while for the rough bed, the primary difference between the 4th-order GC pdf and normal pdf is in the skewness, with the 4th-order GC pdf more skewed to the left. Thus, the conventional use of normal pdf for turbulent velocity would result in an overestimation of kurtosis for the smooth bed but an underestimation of skewness for the rough bed. To further investigate the distribution effect, the LN pdfs (with $\overline{u}_b$ and σ_u identical to the values specified to the GC pdfs) are also illustrated in Fig. 5. It is revealed that both the skewness and kurtosis of the LN pdfs are higher than those of the corresponding GC pdfs, leading to an overestimation of $f_u(u_b)$ in the lower

near-mean region but an underestimation in the further lower region, and an underestimation in the upper near-mean region but an overestimation in the further upper region. It is speculated that the discrepancies between the observation and PL values predicted with earlier lognormal models (Wu and Lin 2002; Wu and Chou 2003a), shown in Fig. 3, arise from such higher skewness and kurtosis coefficients.

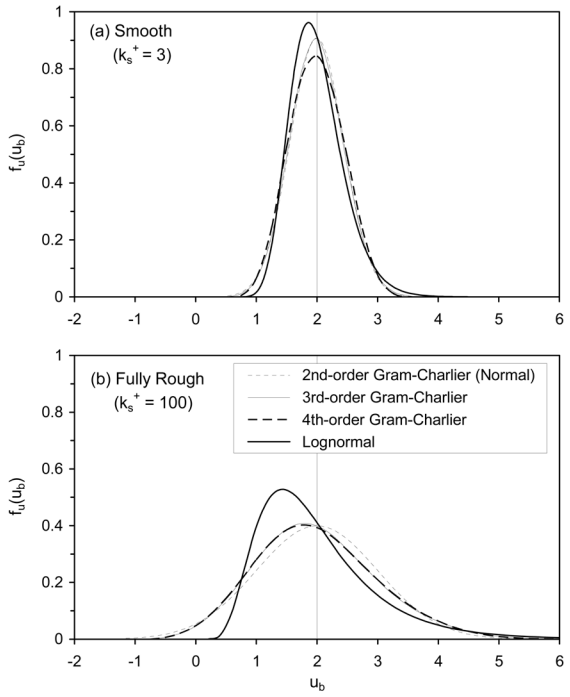

Fig. 5. Comparison of truncated 2nd-, 3rd-, 4th-order GC pdfs and lognormal pdf of u_b for (a) smooth and (b) rough beds

5. 計畫成果自評

本研究內容與原計畫書內容完全相符，預期目標亦全部達成。本研究建立非均勻砂礫啟動之理論模式，利用四階 Gram-Charlier 機率分布描述亂流瞬時速度，以亂流速度跳動之高階相關性(三階動差偏態係數與四階動差峰度係數)納入亂流突暴之效果。本研究之最大貢獻在於全面分析過去30年有關近床有序流結構之實驗研究成果，得到亂流速度跳動之高階(二、三、四階)動差與糙度雷諾數間之定量關係，並用以推求四階 Gram-Charlier 機率分布所需之高階參數。非均勻砂礫之河床隨機結構則採用暴露高度、摩擦高度與遮蔽係數加以量化。理論推導所得之砂礫滾動機率、抬起機率與總啟動機率利用三迴圈計算方法數值求解。計算結果與實驗數據比較顯示，本研究所建立之模式因納入上述諸項因素，較先前以常態分布或對數常態分布為基礎所建立之均勻顆粒啟動模式具有更高之精確度。比較結果亦顯示本研究所建立之模式適用於均勻與非均勻砂礫以及部分運移與全運移狀態。本研究亦發現底床粗糙時四階動差峰度係數之效果不顯著，因此三階與四階 GC pdf 具有相似之結果，但在底床光滑時，則必須利用四階 GC pdf 納入亂流突暴高階相關性之影響。本研究所探討之主題為長期以來序率水理學與輸砂力學極希望解答之問題，至今全世界尚無具體研究成果，因此本計畫之研究成果將成為此領域第一個重要之貢獻，具有非常重要之研究價值與領先國際研究之指標意義。

6. References

[1] Wu, F.-C. (2000), Modeling embryo survival affected by sediment deposition into salmonid spawning gravels: Application to flushing flow prescriptions, *Water Resour. Res.*, 36(6), 1595-1603.

[2] Wu, F.-C., and Y.-C. Lin (2002), Pickup probability of sediment under log-normal velocity distribution, *J. Hydraul. Eng.*, 128, 438-442.

[3] Wu, F.-C., and Y.-J. Chou (2003a), Rolling and lifting probabilities for sediment entrainment, *J. Hydraul. Eng.*, 129, 110-119.

[4] Wu, F.-C., and Y.-J. Chou (2003b), Simulation of gravel-sand bed response to flushing flows using a two-fraction entrainment approach: Model development and flume experiment, *Water Resour. Res.*, 39(8), 1211, doi: 10.1029/2003WR002184.

[5] Wu, F.-C., and K.-H. Yang (2004a), A stochastic partial transport model for

mixed-size sediment: Application to assessment of fractional mobility, *Water Resour. Res.*, 40(4), W04501, doi: 10.1029/2003WR002256.

[6] Wu, F.-C., and K.-H. Yang (2004b), Entrainment probabilities of mixed-size sediment incorporating near-bed coherent flow structures, *J. Hydraul. Eng.*, ASCE, 130(12), 1187-1197.

[7] Wu, F.-C., and Chou, Y.-J. (2004), Tradeoffs associated with sediment-maintenance flushing flows: A simulation approach to exploring non-inferior options, *River Res. Applic.*, 20: 591-604.